

The Phenol Biosensor Based on LDHs / SWNTs Hybrid Materials

Hong-hai Wang^{1,2}, Yan Qin³, Kai-yu Chen³, Huai-guo Xue^{1,3,*}

¹Jiangsu Province Key Laboratory of environment materials and Environment Engineering, Yangzhou University, Yangzhou 225002, P. R. China

²Medical College, Yangzhou Polytechnic College, Yangzhou 225009, P. R. China

³College of Chemistry and Chemical Engineering, Yangzhou University, Yangzhou 225002, P. R. China

*E-mail: chhgxue@yzu.edu.cn

Received: 19 July 2015 / Accepted: 18 October 2015 / Published: 1 December 2015

A novel hybrid material was fabricated with layered double hydroxides (LDHs) and carboxylated Single-walled carbon nanotubes (SWNTs) by electrostatic interaction to fix the dauphin oxidase. Characterization of the samples was carried out using FT-IR spectrophotometer, permeability determination, and electrochemical impedance, respectively. The permeability determination and electrochemical impedance manifested the higher conductivity, larger permeability, and better biocompatibility of the new material, which suggested that this novel material offer a more suitable micro-environment for the survival of enzyme. Results of experiments on response characteristics of the biosensor to five phenolic compounds were given to illustrate the proposed technique, revealing that at the proportion of 25.7:1 (LDHs / SWNTs), the proposed biosensor achieves high sensitivity, low apparent Michaelis constant (0.0065 mM) and wide linear range (7.95×10^{-9} - 3.08×10^{-5} M).

Keywords: Phenol biosensor; LDHs; SWNTs; PPO

1. INTRODUCTION

The determination of phenol and its derivative compounds plays an important role in the environment protection, because these species are toxic wastes in most industries such as oil, dye, polymer and pharmaceutical industries[1]. Among these phenols compounds, chlorophenol is one of the most toxic substrates for humans and aquatic organisms. Therefore, the monitoring of chlorophenol is significant. There have been several methods for chlorophenol determination such as gas chromatography[2], high performance liquid chromatography[3], gas chromatography-Mass spectrometry[4], capillary electrophoresis[5] and electrochemical methods[6]. However, spectrometric

and chromatographic methods require high-cost equipment, complicated sample pretreatment and professional operation procedures. Hence, a simple, fast and selective approach is of eager need for chlorophenol detection. In recent years, electrochemical sensors and biosensors have become prevailing assays for phenol determination. Enzyme-based biosensors are the simple and convenient tool for phenol determination, due to their high selectivity and sensitiveness. For enzymatic sensor, the selection of enzymes also plays a key role in the performance of the as-obtained sensors. Several enzymes such as polyphenol oxidase[7], tyrosinase[8], laccase[9] and horseradish peroxidase[10] had been employed to fabricate enzymatic phenol sensor.

Among the above mentioned enzymes, polyphenol oxidase (PPO), as a kind of copper (II) protein, is abundant in plants, microorganisms, and animals. Under In the presence of oxygen conditions, ortho-hydroxylation reaction was catalyzed by PPO and PPO oxidized to catechol-adjacent-benzene-two-quinone. The reaction mechanism of PPO biosensor is as follows: under aerobic conditions, substrate phenol was amenable to ortho hydroxylation reaction of catechol in the presence of PPO, and then the adjacent benzene two quinone in catalytic role of PPO was further oxidized[11]. It is reported the carrier materials for immobilized enzyme were diverse, such as graphite[12], Al₂O₃ sol-gel film[13], inorganic nano-materials[14], inorganic clay[15], organic polymers[16], and carbon nanotubes[17]. Our previous study had introduced this biopolymer to the surface of clay modified biosensor and obtained dramatically enhanced activity and perfect stability of PPO when it was immobilized in a laponite / chitosan nanocomposite matrix[15]. In recent years, as a class of two-dimensional nanostructured anionic clays, inorganic layered double hydroxides (LDHs) have been widely used in catalysis, separation science, drug delivery, and many other environmental-related fields. Owing to the intrinsically, excellent properties, LDHs have been demonstrated as a promising enzyme immobilization matrix[18, 19].

The latest two decades have witnessed growing attention to carbon nanotubes (CNTs), since it was discovered in 1991 by Iijima[20]. Owing to the nanometric size, higher electrical conductivity, strong adsorptive ability, good mechanical strength, excellent biocompatibility, minimization of surface fouling, and good electrocatalytic properties, CNTs have been widely used in the biosensor fields[21-23]. In particular, single-walled carbon nanotubes (SWNTs) modified biosensor could achieve strong response even at low potential, which demonstrated the excellent electrocatalytic activity of SWNTs and SWNTs based biosensor could exhibit excellent performance such as a wide linear range and fast response time[24]. The advantages of SWNTs including high electrical conductivity, large surface area, and easy electron transfer enables SWNTs to be suitable for the preparation of biosensor.

This article described the preparation of phenol biosensors using single-walled carbon nanotubes and hybrid hydrotalcite-like materials as the immobilized enzyme material. With the addition of some carboxylated SWNTs in simple inorganic clay LDHs, a quantity of inorganic hybrid materials were formed, which not only combined the superiorities of LDHs and SWNTs, but also improved the electron transport ability of the biosensor and maintained its stability.

2. EXPERIMENTAL SECTION

2.1 Materials and methods

Polyphenol oxidase (PPO) (EC 1.14.18.1) from mushroom (807 U mg⁻¹) was purchased from Amresco. Layered double hydroxides (LDHs) was synthesized by coprecipitation method developed by De Roy et al [25]. Single-walled carbon nanotubes (SWNTs, 1-2 nm diameter) were purchased from Aldrich Chemical Co. Preparation of all other reagents is similar to the literature[15].

2.2 Apparatus.

All electrochemical studies were performed on a CHI 660a electrochemical workstation (Shanghai Chenhua Instruments, China) with a conventional three-electrode system using a glassy carbon electrode as the working electrode, a Pt foil electrode as the counter electrode, and a saturated calomel electrode (SCE) as the reference electrode. A glassy carbon electrode (3 mm in diameter) was carefully polished with 0.05 μm alumina particles on silk and rinsed thoroughly with distilled water, followed by drying in air before use. All measurements were carried out in a thermostated cell containing PBS at 25 °C. The apparatus used for determining the current response was a PC-1 precise potentiostat. Fourier transform infrared (FT-IR) spectra of the samples were measured on a pressed pellet with KBr, employing a Tensor 27 spectrometer (Bruker, Germany). The surface morphology of biofilm was observed by the scanning electron microscopy (SEM-FES, S-4800, Hitachi, Japan). Electrochemical impedance spectra (EIS) measurements were conducted using an Autolab/PG-STAT30 (Eco Chemie, Netherlands) with a three-electrode system[15]. Enzyme electrode was fabricated experimental instrument for KQ 300 type VDE dual frequency NC Ultrasonic (Kunshan ultrasonic instruments Co., Ltd.), 90 magnetic stirrer (Shanghai Luxi Analytical Instrument Factory Co., Ltd.), adjustable micropipette (Shanghai Power Equipment Co., Ltd), and pH211 pH (Shanghai Precision Instrument Co., Ltd.).

2.3 Carboxylation of SWNTs

According to the literature [26-27], SWCNTs were taken to carboxylation so as to introduce negative charges on its surface. A certain amount of concentrated nitric acid was added into a weighed amount of the SWCNTs, and subsequently heated to 110 °C under refluxing for 3h. After cooled down to room temperature, the mixture was washed with de-ionised water repeatedly. Finally, the resulting precipitates was filtered and dried for used under ambient conditions. And carboxylated SWNTs was obtained.

2.4 Preparation of Phenol Biosensor

Carboxylated SWNTs was uniformly dispersed tetrahydrofuran (THF) to produced an aqueous solution of 0.5 mg mL⁻¹ through mechanical ultrasonication. Laponite suspension (2 mg mL⁻¹) was

prepared twice in distilled water removing carbon dioxide, and stirred overnight. The de-ionised water was used to prepare the appropriate amount of polyphenol oxidase (PPO) solution (4 mg mL^{-1}).

A certain amount of LDHs and SWNTs suspension (25.7:1) hybrid was processed with ultrasound after a certain time, and enzyme solution was added into the quantitative mixing. The aqueous mixtures of different proportions (for example, containing $13.1 \mu\text{g}$ LDHs, $0.5 \mu\text{g}$ SWNTs, and $13.6 \mu\text{g}$ PPO) was cast on the surface of the glassy carbon electrode and allowed to dry naturally. The resulting electrode was placed in saturated glutaraldehyde vapor at room temperature for 15 minutes in order to induce the chemical cross-linking of the entrapped enzyme molecules. Before use, the enzyme electrode was rinsed under stirring for 20 minutes with buffer solution. Biological electrode was stored at 4°C in a refrigerator when dried.

3. RESULTS AND DISCUSSION

3.1 FT-IR spectra of Phenol biosensors

FT-IR spectroscopy, which could provide some useful information on the structure and conformation of the polyphenol oxidase and hybrid materials, were employed to investigate the existing state. We used infrared spectroscopy to study the interactions between the polyphenol oxidase and hybrid materials. The FT-IR spectra of LDHs / SWNTs (a), pure PPO (b), and LDHs / SWNTs / PPO (c) were shown in Figure 1. The stretching vibrations of various chemical bonds is similar to the literature[15]. Therefore, the LDHs / SWNTs hybrid materials with immobilized enzyme were in favor of maintain the maximum enzyme activity.

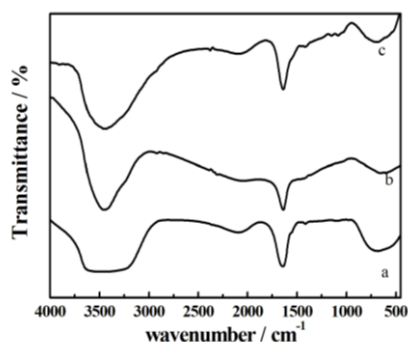


Figure 1. FT-IR spectra of (a) pure PPO, (b) LDHs / SWNTs, and (c) LDHs / SWNTs / PPO

3.2 Morphology of the composite films

The surface morphologies of the membranes were observed via SEM. The images a, b, c and d in Figure 2 exhibited the typical morphologies of pure LDHs, pure SWNTs, LDHs / SWNTs, and LDHs / SWNTs / PPO membranes, respectively. The image a showed loose lamellar and hexagon structures of pure LDHs. The morphology b displayed tubular shape of the pure SWNTs, irregular arrangement of the electrode surface. Graph c was the morphology of LDHs and SWNTs hybrid

material, implying that the hybrid material of SWNTs and LDHs had been intimately mixed together. Graph d was the morphology of LDHs / SWNTs / PPO hybrid membranes. It could be seen in the figure that the enzyme had been successfully embedded in hybrid materials, showing the enzyme like dense sponge deposition in the composite layer space and interaction. Thus the polyphenol oxidase was effectively immobilized onto the LDHs / Laponite composites. The composite membrane could provide a three dimensional structure as the carrier, thereby the enzyme could be tightly embedded in the carrier, which effectively prevented the leakage of enzyme molecules from the film at the same time, and enhanced the charge transfers between the membrane and electrode interface. This was a very important factor in design of high sensitivity of the sensor device.

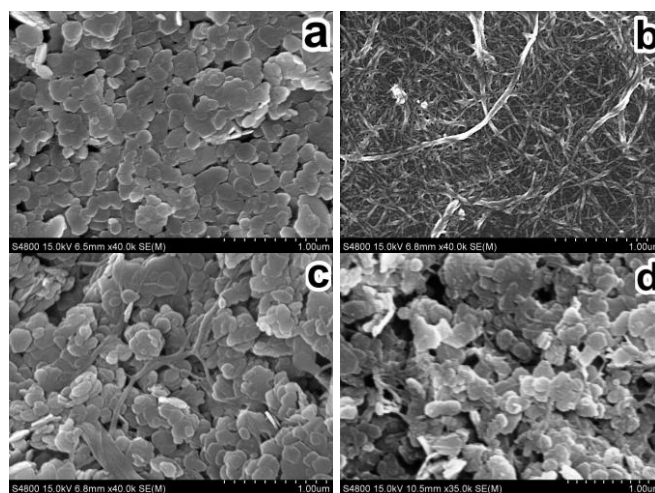


Figure 2. SEM images of LDHs (a), SWNTs (B), LDHs / SWNTs (25.7:1, w/w) (C) and PPO / LDHs / SWNTs (26.7:25.7:1, w/w/w) (D) films

3.3 Electrochemical impedance spectroscopy (EIS)

The electrochemical impedance method was designed to further study the performance of LDHs / SWNTs / PPO biosensor. As a powerful tool for studying the interface properties of surface-modified electrodes, electrochemical impedance spectroscopy (EIS) could be used to structure the electrode system and research on the electrode interface process mechanism, studying on mechanical process and interface process and quantitative. Therefore this experiment was to use the definition of AC impedance of the modified electrode surface. The charge transfer resistance (R_{ct}) of the electrode surface was an important parameter for describing the interfacial properties of the electrode.

Figure 3 displayed the Nyquist plots of the impedance spectroscopy of bare GCE (a), SWNTs (b), LDHs (c), LDHs / SWNTs (d), and LDHs / SWNTs / PPO (e). EIS includes a semicircular part and a linear part. The semicircular part is caused by the charge transfers between and the diameter is equivalent to the R_{ct} , while the linear part is caused by the diffusion of warburg. The R_{ct} of bare GCE, SWNTs, LDHs, LDHs / SWNTs, and LDHs / SWNTs / PPO were 484 Ω , 419 Ω , 5646 Ω , 3872 Ω , and 20980 Ω , respectively. The increase in R_{ct} Indicated that the macromolecular structure of PPO might be propitious to the electron-transfer and Was successfully fixed[15].

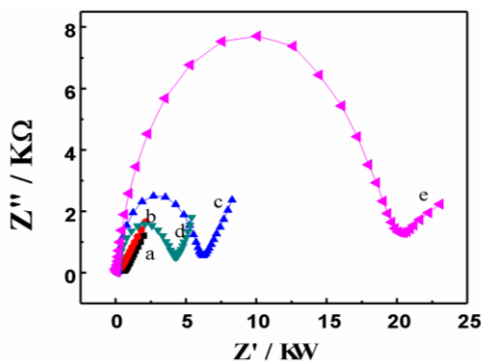


Figure 3. Nyquist plots of EIS for GCE (a), SWNTs (b), LDHs (c), LDHs / SWNTs (d), and LDHs / SWNTs / PPO (e) films in $[\text{Fe}(\text{CN})_6]^{3-/4-}$.

3.4 Permeability of LDHs / SWNTs / PPO electrodes

The permeability of biofilm electrode surface was closely related to the performance of phenol biosensors [28-30]. Therefore the permeability of LDHs / SWNTs / PPO biological membrane was investigated by rotating disk electrode voltammetry. Experiments were performed using 2mM hydroquinone. Figure 4 manifested the curves of LDHs / SWNTs / PPO biofilm electrode by linear voltammetry under the different rotational speeds at the scan rate of 10 mV s^{-1} . Also, the limiting current (i_{lim}) of LDHs / SWNTs / PPO biofilm electrode enhanced with the increase of the speed.

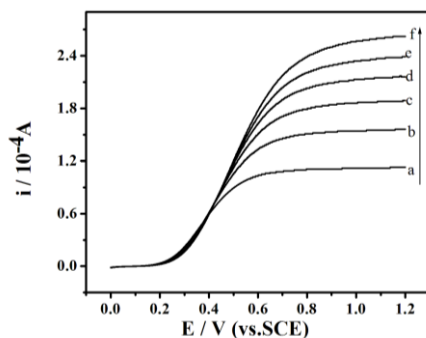


Figure 4. Rotating-disk electrode voltammograms of LDHs / SWNTs / PPO coated on GCE ($d = 5 \text{ mm}$) in the presence of 2 mM hydroquinone in 0.05 M PBS (pH 6.0): (a) 200, (b) 400, (c) 600, (d) 800, (e) 1000, and (f) 1200 rpm/min. Scan rate at 10 mV s^{-1}

According to the relationship between $1/i_{\text{lim}}$ and $1/\omega^{1/2}$ of Koutecky-Levich formula [31-32], the bare electrodes, LDHs / SWNTs, and LDHs / SWNTs / PPO electrode were studied. Figure 6 displayed the diagram of these three different electrodes at different speeds. Three curves of the three electrodes in the same condition showed the linear relation like approximate parallel lines with similar slope. The permeability (P_m) value of the LDHs / SWNTs membrane was $1.84 \times 10^{-2} \text{ cm s}^{-2}$, implying that the film had good permeability and good mass transfer and electronic switching function. When

adding the polyphenol oxidase (PPO), the permeability ($P_m=1.38 \times 10^{-2} \text{ cm s}^{-2}$) decreased since the large molecular structure of PPO hindered the electron transfer.

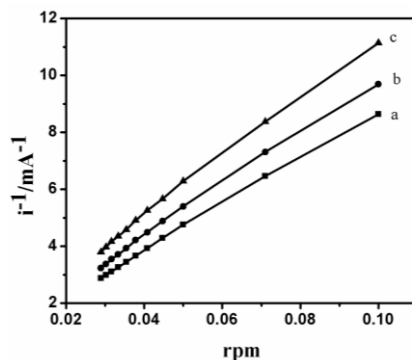


Figure 5. Koutecky-Levich plots for (a) an uncoated electrode, (b) GCE coated with LDHs / SWNTs and (c) GCE coated with PPO / LDHs / SWNTs

3.5 Optimization of the biosensor construction

3.5.1 Effect of weight ratio of LDH / SWNTs on the performance of biosensors.

The composition of LDHs / SWNTs / PPO hybrid materials and responses of the biosensor were studied with catechol as target compounds. The biosensor response of the pure LDHs film ($3722 \text{ mA M}^{-1} \text{ cm}^{-2}$) was smaller than that of LDHs / SWNTs film ($4013 \text{ mA M}^{-1} \text{ cm}^{-2}$). The influence of different weight ratios of LDHs / SWNTs (15:1~40:1, constant amount of PPO ($13.6 \mu\text{g}$)) on the biosensor response to $10 \mu\text{M}$ catechol was examined. Figure 6 showed the current response on LDHs / SWNTs / PPO electrode to $10 \mu\text{M}$ catechol with different weight ratios of LDHs / SWNTs. The optimal weight ratio of LDHs / SWNTs was found to be 25.7:1. This was possibly due to that the biocatalytic activity of PPO was reduced when LDHs and SWNTs weight ratio exceeded a certain proportion. Therefore, the optimal weight ratio of LDHs / SWNTs (25.7:1) was chosen for further experiments.

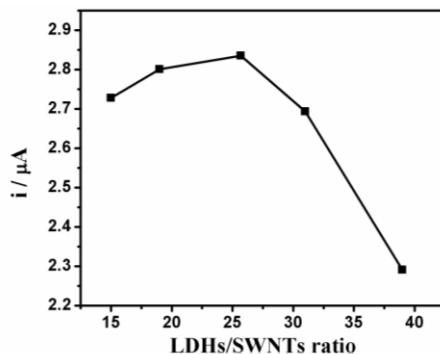


Figure 6. The effect of weight ratio of LDHs / SWNTs at a constant PPO ($13.6 \mu\text{g}$) on the biosensor response to $10 \mu\text{M}$ catechol. ($E_{\text{app}} = -0.20 \text{ V}$, in 0.1 M PBS at $\text{pH } 6.0$, at $25 \text{ }^\circ\text{C}$)

3.5.2 Effect of the thickness of LDH / SWNTs on the performance of biosensors.

Figure 7 showed the influence of film thickness to the biosensor response. If the film thickness increasing, the amount of active PPO and an electrode response increased. However, a thick film might hindered the electron transfer in the diffusion barrier. Therefore, this configuration with 13.6 μg PPO was chosen for further experiments.

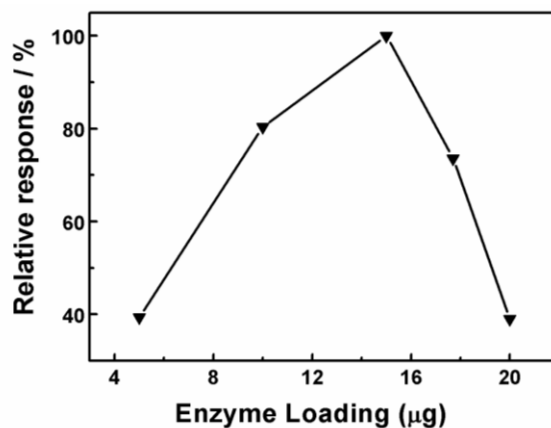


Figure 7. Influence of film thickness to the biosensor response (in 0.1 M PBS at pH 6.0, at 25 °C, $E_{\text{app}} = -0.2$ V) at a constant LDHs / SWNTs / PPO (w/w/w, 3:1:4) ratio

3.5.3 Effect of pH value of the buffer solution on the performance of biosensors.

Biologically active enzyme is very sensitive to pH. Figure 8 showed that the biosensor response increased upon increase of pH to reach maxima at pH 6.0, and then decreased upon further increase of pH to 7.5. The phenomenon is similar to the literature[15]. Therefore, the optimized pH at 6.0 was selected as an experimental variable of enzyme biosensor.

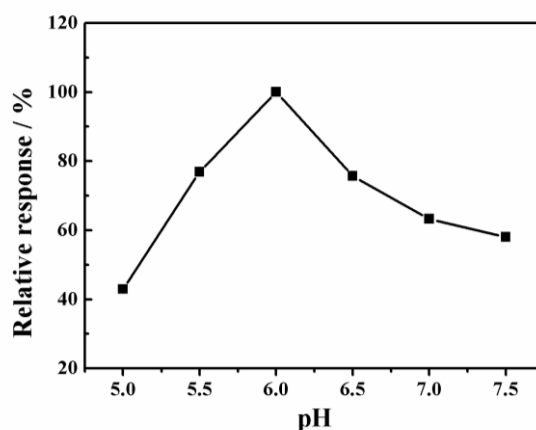


Figure 8. Influence of pH on the biosensor response to 10 μM catechol.

3.5.4 Effect of the operating potential on the response currents of the LDHs / SWNTs / PPO biosensors.

Figure 9 displayed the effect of the operating potential on the response currents of the LDHs / SWNTs / PPO sensor. In the range between -0.30 and 0.00 V, the maximum response was obtained at -0.2 V. However, when the operating potential was larger than -0.2 V, the current response of the biosensor decreased. Moreover, low operating potential could minimize interferences from electroactive species. Therefore, the operating potential of -0.2V was selected for further experiments.

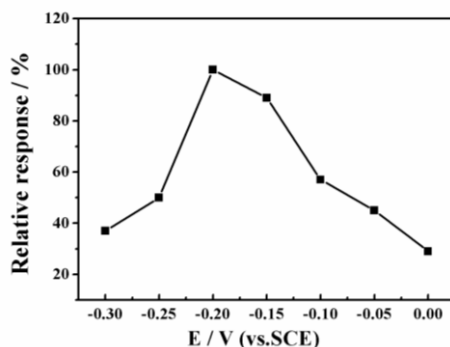


Figure 9. The effect of operating potential on the biosensor response to 10 μ M catechol. (E_{app} = -0.2 V, in 0.1M PBS at pH 6.0, at 25 $^{\circ}$ C)

3.5.5 Effect of temperature on the performance of biosensors

The thermal stability of the bioelectrode was also studied in figure 10. Before amperometric detection, the LDHs / SWNTs / PPO biosensors were immersed into the buffer solution at different temperatures for 20 min. In the range between 5 $^{\circ}$ C and 40 $^{\circ}$ C, the maximum response was obtained at 30 $^{\circ}$ C. This was probably in agreement with the active temperature of OPP enzyme, At the higher temperatures, the OPP enzyme was denatured. In order to obtain the stability of the biosensor at normal temperature, the operating temperature of 25 $^{\circ}$ C was selected for further experiments.

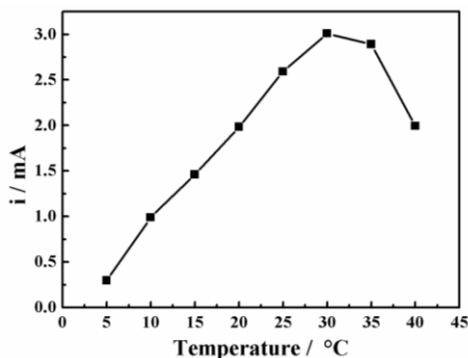


Figure 10. The effect of temperature on the biosensor response in 0.1 M PBS containing 10 μ M catechol with pH 6.0, at 25 $^{\circ}$ C; E_{app} = -0.2 V.

According to the Arrhenius equation ($i(T) = i_0 \exp(-E_a/RT)$) [33], the relationship of $\ln i$ versus T^{-1} in the temperature range of 5–30°C, based on the data, was a straight line, which was displayed in Figure 11. The apparent activation energy (E_a) of the biosensor reaction, calculated from the slope of the straight line, was 34.8 kJ mol⁻¹, which was similar to value of other biosensor immobilized polyphenol oxidase. This indicated that LDHs / SWNTs carrier could provide a good microenvironment for PPO.

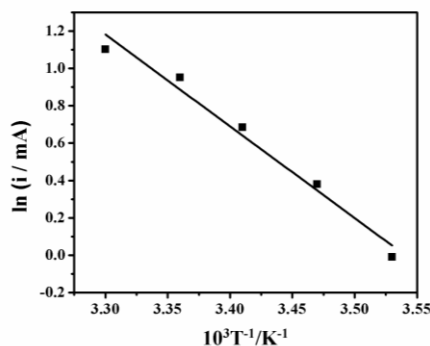


Figure 11. The relationship between $\ln i$ and T^{-1} data

The LDHs / SWNTs / PPO biosensor response current was measured by the amperometric experiments. Figure 12 showed the current response of the LDHs / SWNTs / PPO biosensor for detection of catechol concentration calibration curve under the optimal conditions. The linear range spanned the concentration of catechol from 4.34×10^{-5} to 0.0107 mM with a correlation coefficient of 0.998. The detection limit was 43 nM ($S/N = 3$). Its sensitivity was 4944 mA M⁻¹ cm⁻². However, the sensitivity obtained with the LDHs / PPO electrode (3722 mA M⁻¹ cm⁻²) remained inferior. The apparent Michaelis–Menten constant (K_M^{app}) was evaluated from the electrochemical Lineweaver–Burk plot analysis of the catechol calibration curve (Fig. 12) [15]. Compared with pure LDHs or SWNTs materials, the LDHs / SWNTs hybrid materials have good microenvironment of OPP enzyme, and the LDHs / SWNTs / OPP biosensor has high sensitivity for detection of catechol concentration.

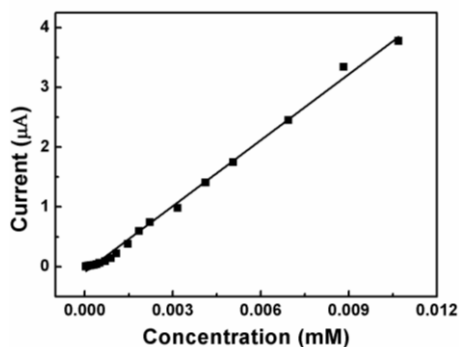


Figure 12. Straight-line showed the linear range of the response (0.1 M PBS, pH=6.0, $E_{app} = -0.2$ V).

There got a straight line through the I^{-1} to $[\text{catechol}]^{-1}$ mapping (Figure 13). The K_M^{app} value of immobilized PPO was 0.023 mM according to the slope and intercept. The K_M^{app} value was lower than that found for the free enzyme insolution (0.28 mM) [34]. The LDHs / SWNTs hybrid materials was found to be good immobilization materials of OPP enzyme form the smaller K_M^{app} value, and the LDHs / SWNTs / OPP biosensor has possessed high enzymatic activity to catechol.

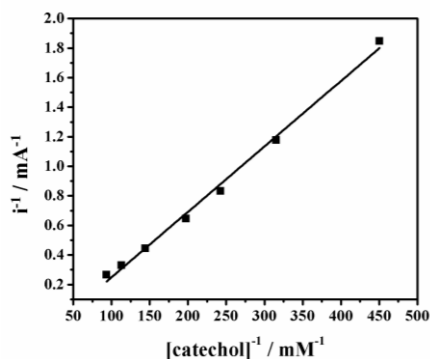


Figure 13. The determination of the apparent Michaelis-Menten constant k'_m for the LDHs / SWNTs / PPO electrode

3.7 Reproducibility and lifetime of the LDHs / SWNTs / PPO biosensors

The reproducibility of the analytical response obtained from five different electrodes constructed by the same procedure was also tested independently. The results indicated that the relative standard deviation (RSD) value for all five electrodes was 4.8 %. The operational stability of the LDHs / SWNTs / PPO biosensors was investigated by successive measurements of its response to 10 μM catechol. Figure 14 showed the LDHs / SWNTs / PPO biosensor response current changed with the growth of time. The LDHs / SWNTs / PPO biosensor retained about 53 % of its original response after 30 days, which indicated that the LDHs / SWNTs hybrid material modified electrode, could maintain the activity of polyphenol oxidase.

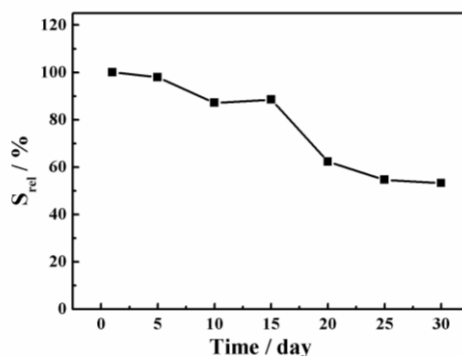


Figure 14. Storage stability for LDHs / SWNTs / PPO bioelectrode testing in 0.1M PBS at pH 6.0, at 25 °C, $E_{\text{app}} = -0.2$ V.

The superior stability of the LDHs / SWNTs / PPO biosensor could be attributed to the good adhesion, the high mechanical strength, and the biocompatible environment of the LDHs / SWNTs hybrid material.

3.8 Response characteristics of the biosensor to various phenolic compounds

Various phenolic compounds were determined by the LDHs / SWNTs / PPO biosensors. Figure 15 showed the calibration curves of five kinds of phenolic compounds concentration. When the substrate concentration was low, the current linearly increased with the increase of substrate concentration. However, at a high concentration of the substrate, the current increased gradually and flattened with the increase of substrate concentration.

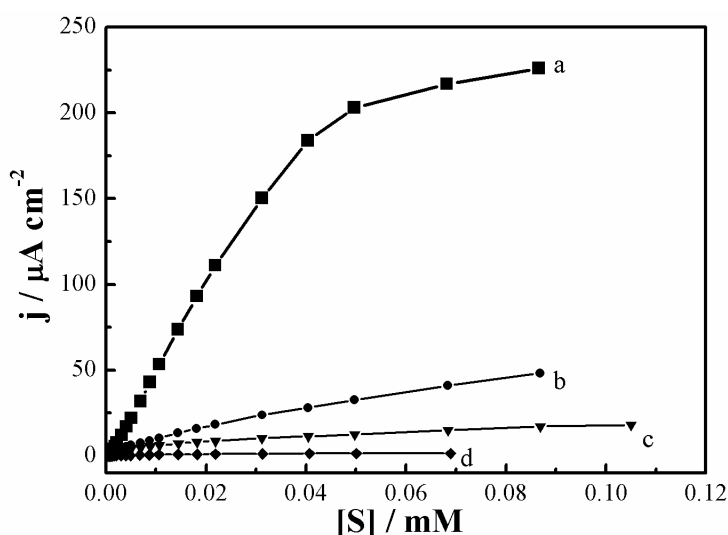


Figure 15. Calibration curves of LDHs / SWNTs / PPO electrode for catechol (a), phenol (b), m-cresol (c), and parachlorophenol (d) in 0.1M PBS (pH 6.0) at 25°C; $E_{app} = -0.20$ V.

The response characteristics of the LDHs / SWNTs / PPO biosensor were studied for five kinds of phenolic compounds. Relevant data were summarized in Table 1. The sensitivity of five kinds of phenolic compounds increased in the following sequence: p-chlorophenol < phenol < m-cresol < p-cresol < catechol. The difference sensitivity of these phenolic compounds might be determined by the characteristics of the immobilization matrix and the hydrophobicity of the molecular space steric hindrance[35]. The K_M^{app} values, 0.0019, 0.0025, 0.0065, 0.012, and 0.023 mM, stated the information on the enzyme-substrate kinetics for the enzyme electrodes, m-cresol, p-cresol, phenol, p-chlorophenol, and catechol, respectively.

Detecting phenol as an example, the linear range and detection limit (see Table 2) were compared with the results of the literature, and the detection limit was approximate or slightly lower.

Table 1. The response characteristics of the LDHs / SWNTs / PPO bioelectrode to phenolic compounds

Phenolic compound	Linear range (M)	Sensitivity ($\text{mA M}^{-1} \text{cm}^{-2}$)	Detection limit (nM)	K_M^{app} (mM)
phenol	7.95×10^{-9} - 3.08×10^{-5}	1532	7.95	0.0065
catechol	4.34×10^{-8} - 1.07×10^{-5}	4944	43	0.023
p-cresol	3.98×10^{-9} - 1.17×10^{-6}	4827	3.98	0.0025
m-cresol	2.18×10^{-8} - 1.07×10^{-6}	3475	3.98	0.0019
p-chlorophenol	1.55×10^{-7} - 1.06×10^{-5}	115.46	155	0.012

Table 2. Comparison of liner range and detection limit for phenol at different electrodes

Type of electrodes	Linear ranges (M)	Detection limit (nM)
GCE/MCN/Tyr biosensor[36]	5.00×10^{-8} - 9.50×10^{-6}	15.00
Tyr/ Al_2O_3 /Sonogel-Carbon electrode [37]	5×10^{-7} - 3×10^{-5}	300
GCE/PVF/Ppy/HRP[38]	0.5×10^{-6} - 1×10^{-5}	23
GCE/ Nano-ZnO /Tyr biosensor[39]	1.5×10^{-7} - 6.5×10^{-5}	50
GCE/LDHs/SWNTs/PPO biosensors	7.95×10^{-9} - 3.08×10^{-5}	7.95

4. CONCLUSIONS

Response characteristics of the LDHs / SWNTs / PPO biosensor to various phenolic compounds were studied. Research results showed that the novel LDHs / SWNTs hybrid material can not only be used to fixed PPO very good, but also to maintain the catalytic activity of the enzyme. This might be attributed to the LDHs / SWNTs hybrid materials providing a very perfect network like structure for the effective immobilization of PPO, but also with the adhesive ability, biocompatibility, and mechanical strength. The phenol biosensor not only showed high sensitivity, good reproducibility and good long-term stability, but also could be determined for many kinds of phenol. It is expected that this LDHs / SWNTs hybrid materials could be widely applied to other biological sensors so as to improve the performance of biosensor.

ACKNOWLEDGEMENTS

The authors are grateful to the financial supports from the National Natural Science Foundation of China (Grant NO. 21173183), 333 Project of Jiangsu Province (Grant NO. BRA2011188), the Priority Academic Program Development of Jiangsu Higher Education Institutions and Key Laboratory of Environment Materials and Environment Engineering of Jiangsu Province (NO. K11035).

References

1. J. Michałowicz, W. Duda, *Pol. J. Environ. Stud.*, 16 (2007)347-362.
2. I. Rodríguez, R. Cela, *TrAC*, 16 (1997)463-475.
3. C. Fan, N. Li, X. Cao, *Food Chemistry*, 174 (2015)446-451.
4. X. Tang, *Huanjing Huaxue*, 33 (2014)2011-2013.
5. S. D. Qi, H. G. Zhang, Q. Zhu, H. L. Chen, Y. L. Dong, L. Zhou, C. L. Ren, X. G. Chen, *Analytical Methods*, 6(2014)1219-1226.
6. X. Bai, X. Huang, X. Y. Zhang, Z.L. Hua, C. F. Wang, Q. Qin, Q. Zhang, *RSC Advances*, 4(2014)13461-13468.
7. S. Seo, V. K. Sharma, N. Sharma, *J. Agric. Food Chem.*, 51(2003) 2837-2838.
8. I. C. Vieira, O. Fatibello-Filho, *Anal. Lett.*, 30(1997)895.
9. A. I. Yaropolov, A.N. Kharybin, J. Emnéus, G. Marko-Varga, L. Gorton, *Anal. Chim. Acta*, 308(1995)137-144.
10. A. Lindgren, J. Emnéus, T. Ruzgas, L. Gorton, G. Marko-Varga, *Anal. Chim. Acta*, 347(1997) 51-62.
11. J. Wang, L. Fang, D. Lopez, *Analyst*, 119(1994)455-458.
12. György Marko-Varga, Jenny Emnéus, Lo Gorton, Tautgirdas Ruzgas, *TrAC*, 14(1995)319.
13. M. Sánchez-Paniagua López, F. Tamimi, López-Cabarcos, B. E. López-Ruiz, *Biosens. Bioelectron*, 24(2009)2574-2579.
14. P. Dykstra, J. J. Hao, S.T. Koev, G. F. Payne, L. L. Yu, R. Ghodssi, *Sens. Actuators B*, 138(2009) 64-70.
15. Q. Fan, D. Shan, H. G. Xue, Y. Y. He, S. Cosnier, *Biosens. Bioelectron*, 22(2007)816-821.
16. Q. Ameer, S. B. Adeloju, *Sens. Actuators B*, 140(2009)5-11.
17. S. Maghsoodi, Z. Gholami, H. Chourchian, Y. Mortazavi, A. A. Khodadadi, *Sens. Actuators B*, 141(2009)526-531.
18. J. M. Gong, Z. Q. Guan, D. D. Song, *Biosens. Bioelectron*, 39(2013)320-323.
19. D. Shan, Y. N. Wang, M. J. Zhu, H.G. Xue, S. Cosnier, C.Y. Wang, *Biosens. Bioelectron*, 24(2009)1171-1176.
20. S. Iijima, *Nature*, 354(1991)56-58.
21. Y. M. Yan, O. Yehezkeli, I. Willner, *Chem. Eur. J.*, 13(2007)10168-10175.
22. Y. Liu, J. Lei, H. Ju, *Talanta*, 74(2008)965-970.
23. X. Yu, B. Munge, V. Patel, G. Jensen, A. Bhirde, J. D. Gong, S. N. Kim, J. Gillespie, J. S. Gutkind, J. S. Rusling, *J. Am. Chem. Soc.*, 128(2006)11199-11205.
24. A. K. Upadhyay, S. M. Chen, T. W. Ting, Y. Y. Peng, *Int. J. Electrochem. Sci.* 6(2011)3466-3482.
25. M. L. Occelli, H. Robson, *Expanded clays and other microporous solids*, New York, Springer (1992).
26. L. H. Niu, Y. W. Tang, F. S. Zhang, *Chem.*, 72(2009)100-104.
27. L. J. Li, C. D. Chen, H. Cheng, Z. Cai, L. Zhong, S. G. Li J. L. Wu, *J. Instrumental Anal.*, 28 (2009) 37-43.
28. D. Shan, S. Cosnier, C. Mousty, *Anal. Chim.* 75(2003)3872-3879.
29. D. Shan, C. Mousty, S. Cosnier, *Anal. Chim.* 76(2004)178-183.
30. Z. H. Dai, M. Fang, J. C. Bao, H. S. Wang, T. H. Lu, *Anal. Chim. Acta*, 591(2007)195-199.

31. D. A. Gough, J. K. Leypoldt, *Anal. Chem.*, 51(1979)439-443.
32. L. N. Wu, M. McIntosh, X. J. Zhang, H. X. Ju, *Talanta*, 74(2007):387-392.
33. R. A. Kamin, G. S. Wilson, *Anal. Chem.*, 52(1980)1198-1205.
34. R. S. Brown, K. B. Male, J. H. Luong, *Anal. Biochem.*, 222(1994)131-139.
35. B. Q. Wang, S. Dong, *J. Electroanal. Chem.*, 487(2000)45-50.
36. Y. Y. Zhou, L. Tang, G. M. Zeng, J. Chen, Y. Cai, Y. Zhang, G. D. Yang, Y. Y. Liu, C. Zhang, W. W. Tang, *Biosens. Bioelectron.*, 61(2014)519-525.
37. H. Zejli, J. L. Hidalgo-Hidalgo de Cisneros, I. Naranjo-Rodriguez, B. H. Liu, K. R. Temsamani, J. L. Martya, *Anal. Chim. Acta*, 612(2008)198-203.
38. M. Topcu Sulak, E. Erhan, B. Keskinler, *Appl. Biochem. Biotechnol.*, 160(2010)856-867.
39. Y. F. Li, Z. M. Liu, Y. L. Liu, Y. H. Yang, G. L. Shen, R. Q. Yu, *Anal. Biochem.*, 349(2006)33-40.

© 2016 The Authors. Published by ESG (www.electrochemsci.org). This article is an open access article distributed under the terms and conditions of the Creative Commons Attribution license (<http://creativecommons.org/licenses/by/4.0/>).